Journal of Solid State Chemistry 187 (2012) 109–113

Contents lists available at SciVerse ScienceDirect

Journal of Solid State Chemistry

journal homepage: www.elsevier.com/locate/jssc

Luminescence properties of core-shell structured SiO_2@$CaMoO_4$:Eu^{3+} phosphor

Xiaoxia Ju [a], Xueming Li [a,*], Yuling Yang [a], Wulin Li [b], Chuanyi Tao [b], Wenlin Feng [a,c,d]

[a] College of Chemistry and Chemical Engineering, Chongqing University, Chongqing 400044, China
[b] Key Laboratory for Optoelectronic Technology and Systems, Ministry of Education, College of Optoelectronic Engineering, Chongqing University, Chongqing 400044, China
[c] Department of Applied Physics, Chongqing University of Technology, Chongqing 400054, China
[d] International Centre for Materials Physics, Chinese Academy of Sciences, Shenyang 110016, China

ARTICLE INFO

Article history:
Received 18 July 2011
Received in revised form
26 December 2011
Accepted 27 December 2011
Available online 8 January 2012

Keywords:
$CaMoO_4$:Eu^{3+}
SiO_2
Sol-gel method
Luminescence

ABSTRACT

Uniform SiO_2@$CaMoO_4$:Eu^{3+} red phosphor has been synthesized by sol-gel method, and its luminescence properties have been studied by fluorescence spectrometer. The structure and morphology of the SiO_2@$CaMoO_4$:Eu^{3+} red phosphor have been investigated by transmission electron microscopy (TEM), scanning electron microscopy (SEM) and energy dispersive spectroscopy (EDS), X-ray diffraction (XRD), and FT-IR spectrometer. Results indicate that phosphor particles have a core-shell structure and the thickness of the SiO_2-shell is about 60 nm. In addition, the luminescent intensity of SiO_2@$CaMoO_4$:Eu^{3+} red phosphor has been greatly enhanced with respect to $CaMoO_4$:Eu^{3+} phosphor. But the lifetime τ value of SiO_2-coated $CaMoO_4$:Eu^{3+} is slightly smaller than that of non-coated $CaMoO_4$:Eu^{3+}.

1. Introduction

Phosphor-converted white-light emitting diodes (W-LEDs) have become the main lighting source in 21st century because of their advantages of energy-saving, pollution-free and so on [1]. Red phosphors are significant components of tricolor (red, green and blue) phosphors, which are very important for realization of W-LEDs. However, commercial red phosphors such as Y_2O_2S:Eu^{3+} exist some disadvantages of low light-emitting efficiency, large light decay and unstable chemical property which seriously affect the lifetime and efficiency of W-LEDs [2]. Compared with Y_2O_2S:Eu^{3+} red phosphor, $CaMoO_4$:Eu^{3+} red phosphor exhibits higher light-emitting efficiency and better color purity. According to the previous literature [3–6], we can know that $CaMoO_4$:Eu^{3+} red phosphor prepared by co-precipitation method have better morphology and luminescent properties than that synthesized by traditional solid-state reaction method.

Though $CaMoO_4$:Eu^{3+} red phosphor synthesized by co-precipitation method hold stronger luminescent intensity and better morphology, they also have the drawbacks of large luminous decay and instability of particles surface. Many studies have reported that those problems can be resolved if inorganic nano-oxide layer is coated on the surface of phosphors [7–9]. Compared with common coating agents, such as Al_2O_3 [10], Y_2O_3 [11], etc. [12,13], SiO_2 is an excellent coating material for its transparency and adhesion. It is easily to form compact SiO_2 layer with good chemical stability on the surface of phosphors. In addition, the silica coating has already been applied to some inorganic particles, and the thin silica layer improves the thermal stability [14,15]. Therefore, SiO_2@$CaMoO_4$:Eu^{3+} red phosphor should deliver good thermal stability. Especially, the effect of the SiO_2-shell on the optical properties of $CaMoO_4$:Eu^{3+} phosphor has never been studied.

In this paper, the layer of SiO_2 film was synthesized by the sol-gel method. It was coated on the surface of the $CaMoO_4$:Eu^{3+} red phosphor prepared by co-precipitation method. In addition, the structure, luminescence properties and thermal stability of SiO_2@$CaMoO_4$:Eu^{3+} red phosphor are also systematically studied in this paper.

2. Experimental

2.1. Synthesis of $CaMoO_4$:Eu^{3+}

$CaMoO_4$:Eu^{3+} red phosphor was prepared by co-precipitation method according to the previous literature [16]. $Eu(NO_3)_3 \cdot 5H_2O$ (A.R.), $(NH_4)_6Mo_7O_{24} \cdot 4H_2O$ (A.R.), $Ca(NO_3)_2 \cdot 4H_2O$ (A.R.), NH_4HCO_3 (A.R.), $NH_3 \cdot H_2O$ (A.R.), HNO_3 (A.R.) and PEG20000 (A.R.) were used as the starting materials. There PEG20000 is surfactant, and NH_4HCO_3 and $NH_3 \cdot H_2O$ are precipitators. First, stoichiometric amounts of $(NH_4)_6Mo_7O_{24} \cdot 4H_2O$, $Eu(NO_3)_3 \cdot 5H_2O$ and $Ca(NO_3)_2 \cdot 4H_2O$ were

* Corresponding author. Fax: +86 23 65105659 (Office).
E-mail addresses: xuemingli@cqu.edu.cn, juxiaoxia225@126.com (X. Li).

0022-4596/$ - see front matter © 2012 Elsevier Inc. All rights reserved.
doi:10.1016/j.jssc.2011.12.042

dissolved in distilled water under magnetic stirring and heating, then the mixture was dropped into NH_4HCO_3–$NH_3 \cdot H_2O$ precipitator with PEG20000 under continuous stirring and white precipitation generated. After aging, filtration, washing, drying, the white precursor was obtained. Finally, the precursor was presinted at 500 °C for 2 h and calcined at 800 °C for 4 h, and the sample was obtained.

2.2. Synthesis of SiO_2@$CaMoO_4$:Eu^{3+}

SiO_2@$CaMoO_4$:Eu^{3+} red phosphor was synthesized according to the following procedure: TEOS (A.R.), CH_3CH_2OH (A.R.) and deionized water were mixed uniformly at volume ratio of 1:3:4 and the pH value of mixture was adjust to 9–10 by dropping $NH_3 \cdot H_2O$. The solution was heated in 85 °C water bath under magnetic stirring. Until the solution turns into gel, a certain amount of $CaMoO_4$:Eu^{3+} were added with continuous stirring. Then the obtained expanding phosphor was ultrasonically dispersed for 5 min. They are dried at 120 °C for 1 h and presinted at 300 °C for 2 h, and SiO_2@$CaMoO_4$:Eu^{3+} red phosphor was got.

2.3. Characterization

The XRD of samples were carried out by X-ray diffraction with Cu$K\alpha$ radiation (λ=0.15405 nm). The accelerating voltage and emission current were 40 kV and 30 mA, respectively. FT-IR spectra were performed by MAGNA-IR 550 IR spectrophotometer using the KBr pellet technique. The resolution of the FTIR measurements is 4 cm^{-1}. The morphology of phosphor was characterized by TESCAN VEGAIILMU scanning electron microscope. The surfaces structure of phosphor particles were studied by Tecnai G2F20 field emission transmission electron microscope. The composition of sample was analyzed by INCA energy-dispersive X-ray spectrometer (EDS). The photoluminescence was characterized by RF-5301 fluorescence spectrometer with the xenon lamp as excitation source. The fluorescence decay time was taken by Jobin-Yvon Fluorolog-3-tau system, which was equipped with a 450 W Xe lamp for steady-state measurement and a 50 W flash lamp for frequency domain dynamic measurement. All the measurements were recorded at room temperature.

3. Results and discussion

3.1. The microstructure and composition analysis of SiO_2@$CaMoO_4$:Eu^{3+} red phosphor

The SEM and TEM images of naked $CaMoO_4$:Eu^{3+} microspheres and SiO_2@$CaMoO_4$:Eu^{3+} microspheres are given in Fig. 1. It shows that the surfaces of naked $CaMoO_4$:Eu^{3+} spheres are smooth without attachments in Fig. 1a and b, while SiO_2@$CaMoO_4$:Eu^{3+} spheres have a core-shell structure, the silica shell is clearly visible in Fig. 1c and d, and the thickness of the silica shell is about 60 nm. As shown in Fig. 1d, the nano-layer continuously disperses on the surface of phosphor and there is no nuclear particle of SiO_2 in the gel layer [17]. This is because the appropriate reaction time makes the SiO_2 nano-layer

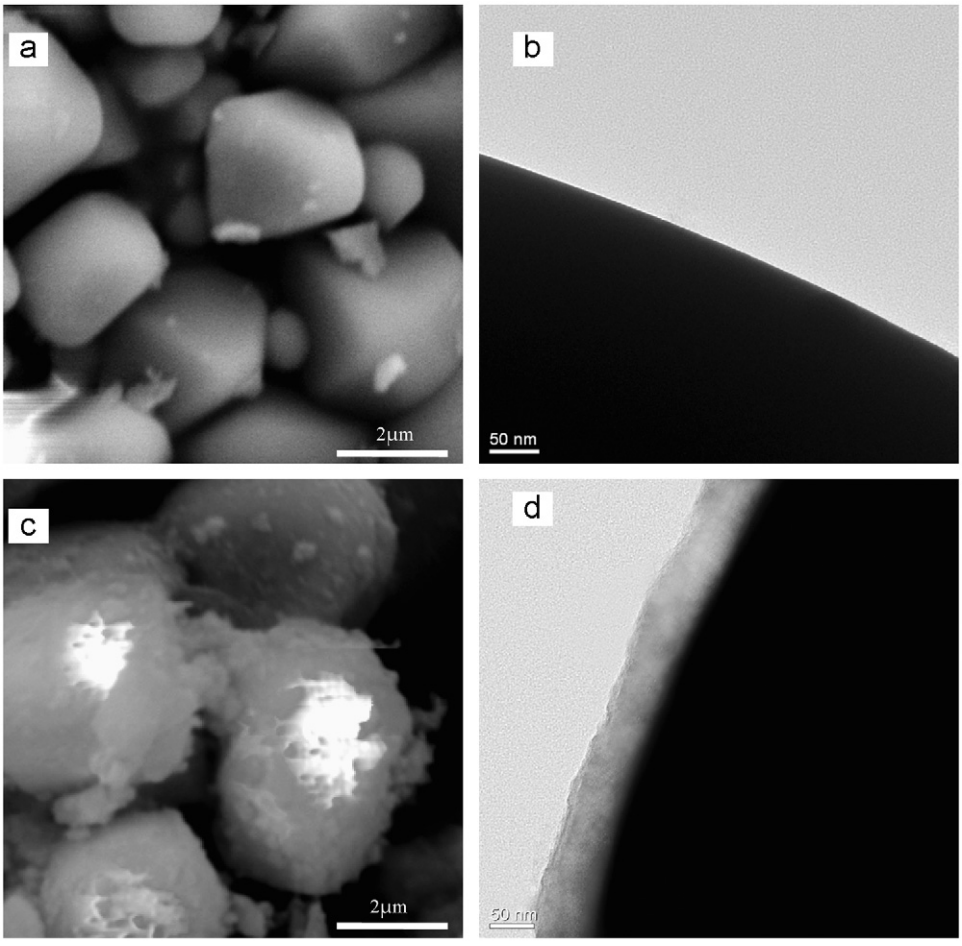

Fig. 1. SEM and TEM images of $CaMoO_4$:Eu^{3+} (a, b) and SiO_2@$CaMoO_4$:Eu^{3+} (c, d).

homogeneously adsorbed on the surface of $CaMoO_4:Eu^{3+}$ microsphere and forms continuous SiO_2 nano-layer with uniform thickness. Fig. 2 shows EDS spectra of $CaMoO_4:Eu^{3+}$ and $SiO_2@CaMoO_4:Eu^{3+}$ red phosphor, respectively. As seen from Fig. 2a, no Si signal is detected in the EDS spectra of uncoated $CaMoO_4:Eu^{3+}$. While for the coated $CaMoO_4:Eu^{3+}$, it is clearly shown from Fig. 2b that Ca, Mo, O and Si peaks are at the normal energies, which indicate that the coated layer is SiO_2. Therefore, based on the TEM and EDS results, it can be confirmed that the $CaMoO_4:Eu^{3+}$ microspheres were coated by a uniform silica shell.

3.2. The XRD analysis of $SiO_2@CaMoO_4:Eu^{3+}$ red phosphor

The XRD patterns of SiO_2, $SiO_2@CaMoO_4:Eu^{3+}$ and $CaMoO_4:Eu^{3+}$ are shown in Fig. 3. It can be found that the XRD peaks of these two samples are quite similar, which implies that crystal structure of $CaMoO_4:Eu^{3+}$ red phosphor is not influenced by SiO_2 nano-layer, $SiO_2@CaMoO_4:Eu^{3+}$ red phosphor is still single tetragonal scheelite structure. It also can be seen that the phase of SiO_2 was not detected in the SiO_2-coated $CaMoO_4:Eu^{3+}$ samples, which may be due to that the silica has an amorphous network [14,18].

3.3. The FT-IR analysis of $SiO_2@CaMoO_4:Eu^{3+}$ red phosphor

Fig. 4 displays FT-IR spectra of SiO_2, $SiO_2@CaMoO_4:Eu^{3+}$ and $CaMoO_4:Eu^{3+}$. With comparison of FT-IR spectra of three samples, it can be obtained that the FT-IR spectra of $CaMoO_4:Eu^{3+}$ and $SiO_2@CaMoO_4:Eu^{3+}$ are similar, except for the absorption peak at 1082.1 cm^{-1} which attributes to stretching vibration absorption of Si–O–Si. Combined with the microstructure, composition and XRD analysis, it proves that the $CaMoO_4:Eu^{3+}$ microspheres surfaces are effectively coated by amorphous SiO_2 layer. The weak adsorption bands at 3450.0 and 1634.3 cm^{-1} are owed to O–H stretching vibration and H–O–H bending vibration absorption for the physically absorbed water on the sample surface. The strong absorption peaks between 912.1 to 805.4 cm^{-1} are assigned to stretching vibration of O–Mo–O in MoO_4^{2-} tetrahedron, and the adsorption peak at 428.6 cm^{-1} corresponds to v_2 bending vibration of Mo–O [19].

3.4. The luminescent property of $SiO_2@CaMoO_4:Eu^{3+}$

Fig. 5 gives the excitation and emission spectra of $CaMoO_4:Eu^{3+}$ and $SiO_2@CaMoO_4:Eu^{3+}$. The spectra show that the peaks

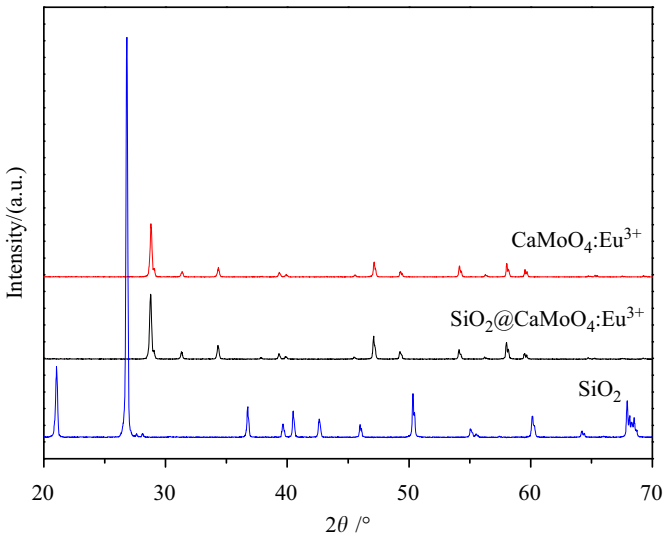

Fig. 3. XRD patterns of SiO_2, $SiO_2@CaMoO_4:Eu^{3+}$ and $CaMoO_4:Eu^{3+}$.

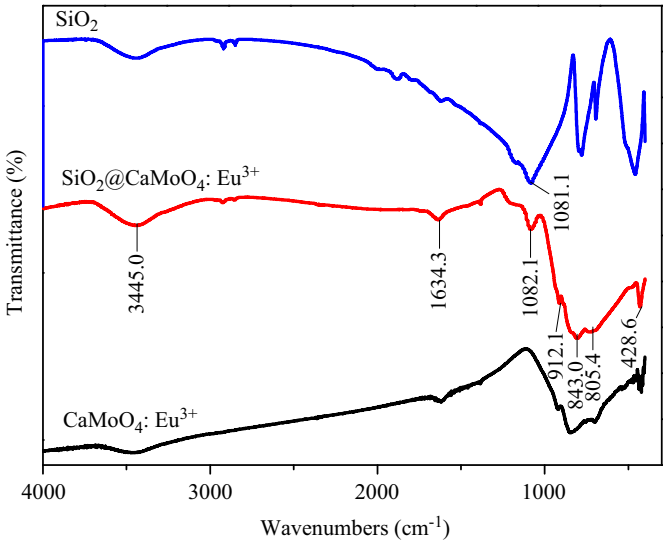

Fig. 4. FT-IR spectra of SiO_2, $SiO_2@CaMoO_4:Eu^{3+}$ and $CaMoO_4:Eu^{3+}$.

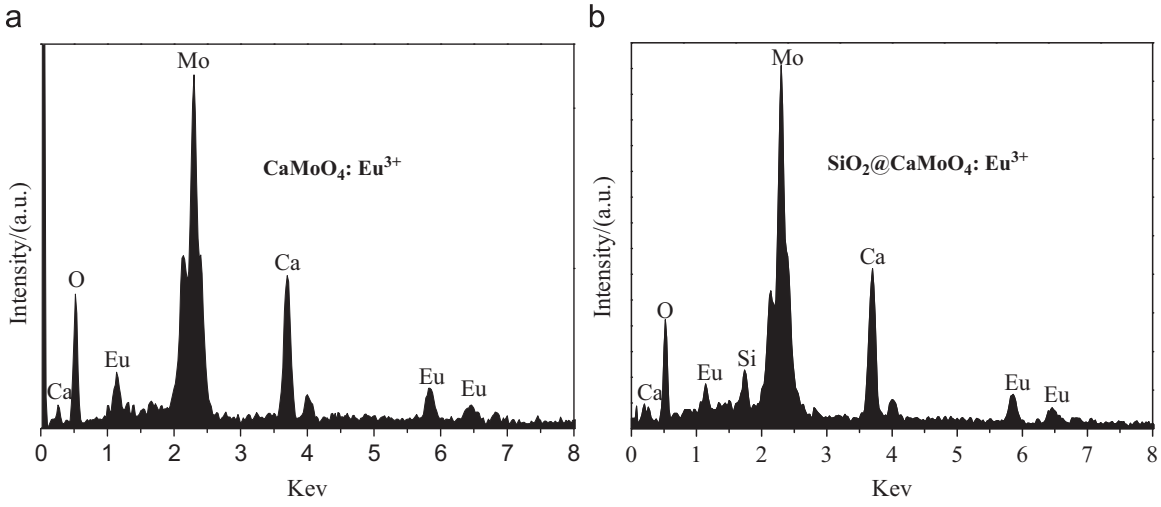

Fig. 2. EDS spectra of $CaMoO_4:Eu^{3+}$ (a) and $SiO_2@CaMoO_4:Eu^{3+}$ (b).

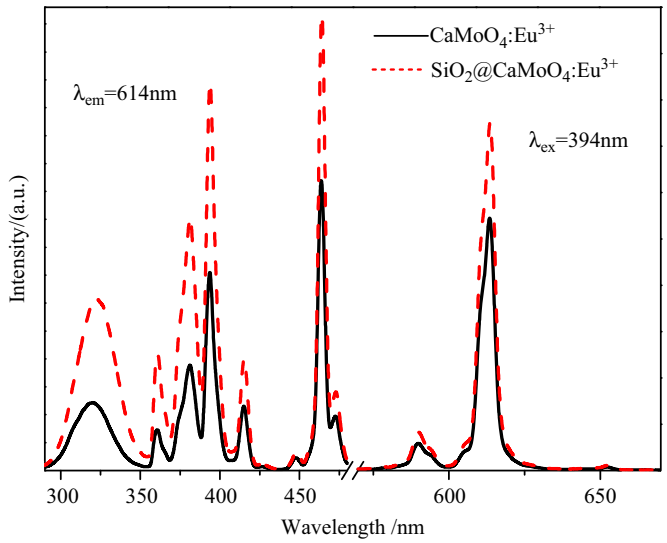

Fig. 5. Excitation and emission spectra of $CaMoO_4:Eu^{3+}$ (solid line) and $SiO_2@CaMoO_4:Eu^{3+}$ (dashed line).

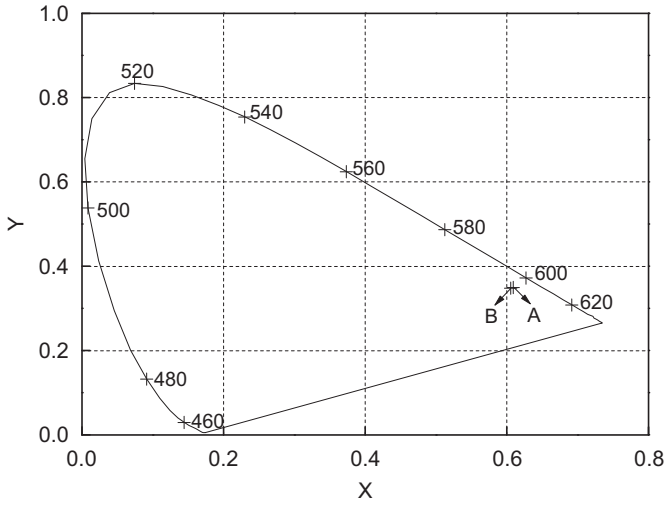

Fig. 6. The measured color coordinates of the $CaMoO_4:Eu^{3+}$ (point A) and $SiO_2@CaMoO_4:Eu^{3+}$ (point B) in the CIE chromaticity diagram.

position of $CaMoO_4:Eu^{3+}$ are not affected by SiO_2 nano-layer. All the peaks are characteristic transition of Eu–O and Eu^{3+}, which also indicates that the SiO_2 nano-layer does not destroy the structure and luminescence properties of $CaMoO_4:Eu^{3+}$ phosphor. Furthermore, the luminescent intensity of $SiO_2@CaMoO_4:Eu^{3+}$ red phosphor is increased largely, which opposites to the report [20] that coating decreases the luminescent intensity of phosphor, indicating that the presence of SiO_2 layer on the surface of phosphor affects the luminescent intensity. This can be interpreted with the reduction of the reflectivity of the excitation UV light from the surface of the $CaMoO_4:Eu^{3+}$ phosphor due to the SiO_2 coating. Considering the refractive index (n) of the air ($n=1.0$), SiO_2 ($n=1.5$) and $CaMoO_4:Eu^{3+}$ phosphors ($n=2.0$), we can easily find that the reflectivity of the UV between air and $CaMoO_4:Eu^{3+}$ surface is about 0.111 while the total reflectivity of air–SiO_2 (0.040) and SiO_2–$CaMoO_4:Eu^{3+}$ (0.020) layers sums to 0.060. Therefore, more excitation UV light is transmitted into the $CaMoO_4:Eu^{3+}$ phosphor by virtue of the SiO_2 coating and thence the luminescent intensity is increased [21–25].

Fig. 6 shows the measured color coordinates of $CaMoO_4:Eu^{3+}$ (point A) and $SiO_2@CaMoO_4:Eu^{3+}$ (point B) phosphor in the CIE chromaticity diagram, respectively. According to Fig. 6, it is shown that point A with chromaticity coordination of (0.609, 0.350) and point B with chromaticity coordination of (0.605, 0.348) both locate in the region of red-orange color, which displays that effect of SiO_2 nano-coating on the chromaticity of $CaMoO_4:Eu^{3+}$ is slightly.

The luminescent intensity of $CaMoO_4:Eu^{3+}$ and $SiO_2@CaMoO_4:Eu^{3+}$ with different calcining time at 500 °C is reported in Fig. 7. The luminescent intensity of phosphors decreased with the calcining time prolonging. The reduction of Eu^{3+} to Eu^{2+} in air atmosphere may be a reason for this. According to the previous literature [26–31], when alkaline earth ions in borates, phosphates or borophosphates are substituted partially and aliovalently by trivalent rare earth ions such as Sm^{3+}, Eu^{3+}, these rare earth ions can be reduced to divalent state by the produced negative charge vacancy V''_M. The matrices must have appropriate structure containing a rigid three-dimensional network of tetragonal AO_4 groups ($A=B$, P). These groups can surround and isolate the produced divalent RE^{2+} ions from the reaction with oxygen. Therefore, this reduction reaction can be carried out even in air at high temperature. Because molybdate anion exists also in the tetrahedral MoO_4

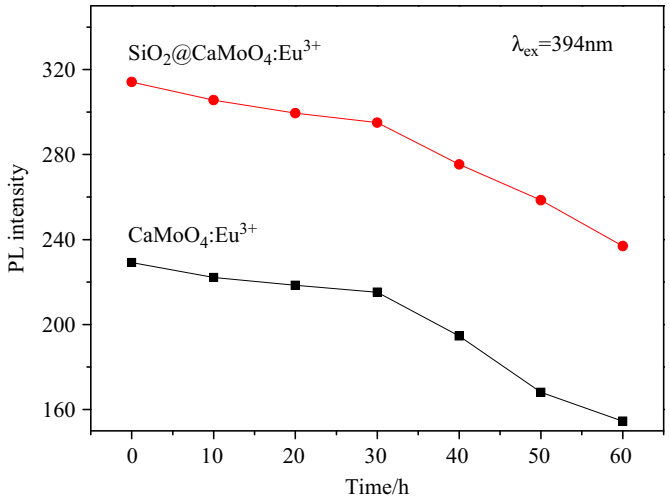

Fig. 7. Luminescent intensity of $CaMoO_4:Eu^{3+}$ and $SiO_2@CaMoO_4:Eu^{3+}$ with different calcining time at 500 °C (λex=394 nm).

unit [32], it is possible that MoO_4 groups can reduce Eu^{3+} into Eu^{2+} even in air at high temperature. The longer the time of $CaMoO_4:Eu^{3+}$ and $SiO_2@CaMoO_4:Eu^{3+}$ calcined at 500 °C, the more Eu^{3+} have been reduced to Eu^{2+}, the lower the intensity of phosphors.

Fig. 8 shows the fluorescence decay curves of non-coated and SiO_2-coated $CaMoO_4:Eu^{3+}$ red phosphors, respectively. The decay curve of non-coated and SiO_2-coated $CaMoO_4:Eu^{3+}$ red phosphors both can be well fitted into a bi-exponential function as $I=I_0\exp(-t/\tau)$, and the lifetime τ values are determined to be 0.46839 and 0.49370 ms, respectively. It is worth noting that the lifetime τ value of SiO_2-coated $CaMoO_4:Eu^{3+}$ is slightly smaller than that of non-coated $CaMoO_4:Eu^{3+}$. Maybe this can be interpreted as follows. Because the lifetimes of the $^5D_0$ excited state of Eu^{3+} ions within $CaMoO_4$ cores are not almost interfered by the outside environments, whereas the lifetimes of Eu^{3+} ions near or on the surfaces of microparticles are greatly disturbed by non-radiative factors such as surface defects, functional groups with high vibration energy and surface contamination [33].

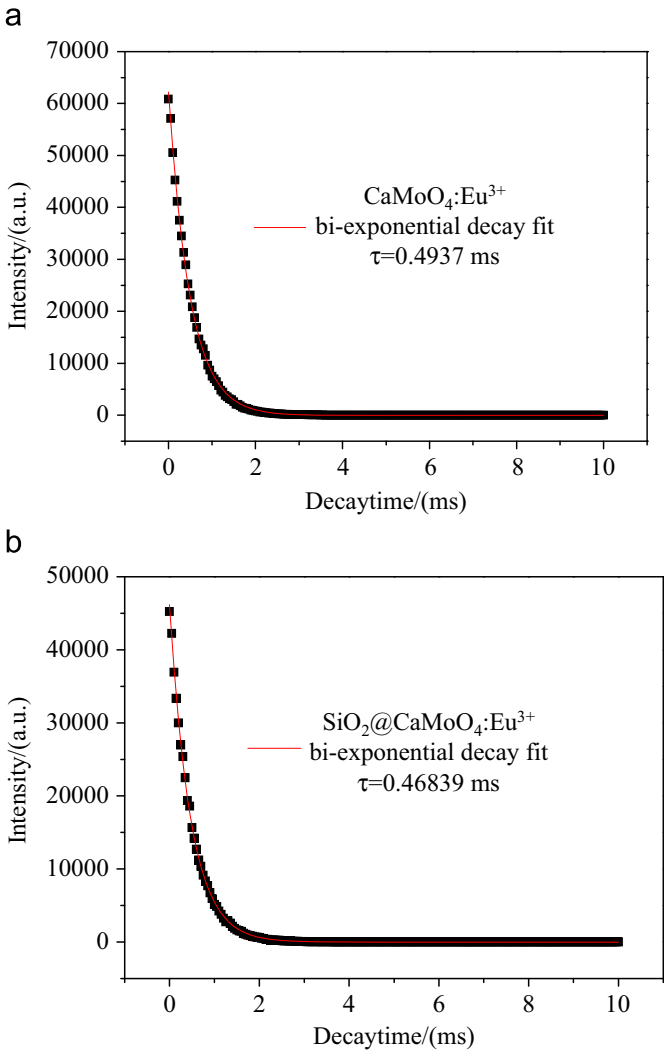

Fig. 8. The normalizing fluorescence decay curves of non-coated (a) and SiO_2-coated $CaMoO_4:Eu^{3+}$ (b) (λex=394 nm, λem=614 nm), and their results fitted by the bi-exponential decay.

4. Conclusions

With NH_4HCO_3–$NH_3 \cdot H_2O$ as mixed precipitator, $CaMoO_4:Eu^{3+}$ red phosphor was successfully prepared by co-precipitation method. The SiO_2 nano-layer with thickness of about 60 nm is successfully coated on the surface of $CaMoO_4:Eu^{3+}$ red phosphor by sol-gel method. The SiO_2 nano-layer cannot destroy the structure of $CaMoO_4:Eu^{3+}$ phosphor, while it greatly improves their luminescent properties. The luminescent intensity of phosphors decreased with the calcining time prolonging at 500 °C, and the lifetime τ values of non-coated and SiO_2-coated $CaMoO_4:Eu^{3+}$ red phosphors are determined to be 0.46839 and 0.49370 ms, respectively.

Acknowledgments

This project is supported by the Innovative Talent Training Project of the Third Stage of "211 Project", Chongqing University (No.S-09103), the Natural Science Foundation of Chongqing (No.2005BA4016), the National Science Foundation for Post-doctoral Scientists of China (No. 20100470811) and the Fundamental Research Funds for the Central Universities (No.CDJXS10122217).

References

[1] T.T. Dong, Z.H. Li, Z.X. Ding, L. Wu, X.X. Wang, X.Z. Fu, Mater. Res. Bull. 43 (2008) 1694–1760.
[2] K.S. Hwang, S. Hwangbo, J.T. Kim, Ceram. Int. 35 (2009) 2517–2519.
[3] L. Yang, L.Q. Zhou, Y. Huang, Z.W. Tang, Mater. Res. Bull. 46 (2011) 239–243.
[4] G.X. Liu, G.Y. Hong, J.X. Wang, X.T. Dong, J. Alloys Compd. 432 (2007) 200–204.
[5] M.M. Haque, H.I. Lee, D.K. Kim, J. Alloys Compd. 481 (2009) 792–796.
[6] Y.L. Yang, X.M. Li, W.L. Feng, W.L. Li, C.Y. Tao, J. Alloys Compd. 505 (2010) 239–242.
[7] Y. Wang, W.P. Qin, J.S. Zhang, C.Y. Cao, J.S. Zhang, Y. Jin, P.F. Zhu, G.D. Wei, G.F. Wang, L.L. Wang, J. Solid State Chem. 180 (2007) 2268–2272.
[8] X.M. Liu, J. Lin, J. Nanopart. Res. 9 (2007) 869–875.
[9] D. Kima, S. Jeong, J. Moon, S.H. Cho, J. Colloid Interface Sci. 297 (2006) 589–594.
[10] M. Jayasankar, S. Ananthakumar, P. Mukundan, W. Wunderlich, K.G.K. Warrier, J. Solid State Chem. 181 (2008) 2748–2754.
[11] W. Park, K. Yasuda, B.K. Wagner, C.J. Summers, Y.R. Do, H.G. Yang, Mater. Sci. Eng. B 76 (2000) 122–126.
[12] R.B. Zheng, X.W. Meng, F.Q. Tang, J. Solid State Chem. 182 (2009) 1235–1240.
[13] H. Kominami, T. Nakamura, K. Sowa, Y. Nakanishi, Y. Hatanaka, G. Shimaoka, Appl. Surf. Sci. 114 (1997) 519–522.
[14] H.Y. Song, Y.M. Leem, B.G. Kim, Y.T. Yu, Mater. Sci. Eng. B 143 (2007) 70–75.
[15] J. Mu, D.Y. Gu, Z.Z. Xu, Mater. Res. Bull. 40 (2005) 2198–2204.
[16] Y.L. Yang, X.M. Li, W.L. Feng, W.J. Yang, W.L. Li, C.Y. Tao, J. Alloys Compd. 509 (2011) 845–848.
[17] L. Poul, S. Ammar, N. Jouini, F. Fievet, J. Sol-Gel Sci. Technol. 26 (2003) 261–265.
[18] S.D. Han, J.D. Kim, K.S. Myung, Y.H. Lee, H. Yang, K.C. Singh, Mater. Chem. Phys. 103 (2007) 89–94.
[19] I.L.V. Rosa, A.P.A. Marques, M.T.S. Tanaka, D.M.A. Melo, E.R. Leite, E. Longo, J.A. Varela, J. Fluoresc. 18 (2008) 239–245.
[20] J.Q. Zhuang, Z.G. Xia, H.K. Liu, Z.P. Zhang, L.B. Liao, Appl. Surf. Sci. 257 (2011) 4350–4353.
[21] I.Y. Jung, Y. Cho, S.G. Lee, S.H. Sohn, D.K. Kim, Y.M. Kweon, Appl. Phys. Lett. 87 (2005) 191908–191910.
[22] S.H. Sohn, J.H. Lee, S.M. Lee, J. Lumin. 129 (2009) 478–481.
[23] H.S. Kim, H.J. Kim, Y.K. Jeoung, S.H. Kim, S.W. Lee, B.K. Jeong, H.H. Lee, B.H. Choi, Solid State Phenom. 375 (2007) 124–126.
[24] C. Enrico, B. Enrico, B. Alessandro, J. Phys.: Condens. Matter 14 (2002) 5221–5228.
[25] I.H. Malitson, M.J. Dodge, R.M. Waxler and W.S. Brower. Annual Meeting of the Optical Society of America, 1971, p. 10.
[26] I. Tale, P. Kulis, V. Kronghauz, J. Luminesc. 20 (1979) 343.
[27] Q. Su, H.B. Liang, T.D. Hu, Y. Tao, T. Liu, J. Alloys Compd. 344 (2002) 132–136.
[28] Z.W. Pei, Q.H. Zeng, Q. Su, J. Phys. Chem. Solids 61 (2000) 9–12.
[29] B.K. Grandhe, V.R. Bandi, K.W. Jang, S.S. Kim, D.S. Shin, Y. Lee, J.M. Lim, T. Song, J. Alloys Compd. 509 (2011) 7937–7942.
[30] M.Y. Peng, Z.W. Pei, G.Y. Hong, Q. Su, Chem. Phys. Lett. 371 (2003) 1–6.
[31 Z. Pei, Q. Zeng, Q. Su, J. Solid State Chem. 145 (1999) 212–215.
[32] Z.J. Zhang, H.H. Chen, X.X. Yang, J.T. Zhao, Mater. Sci. Eng. B 145 (2007) 34–40.
[33] Q. Lü, A.H. Li, F.Y. Guo, L. Sun, L.C. Zhao, Nanotechnology 19 (2008). 205704 (8pp).